Journal of Metals, Materials and Minerals, Vol. 30, No. 3, pp. 9-14, 2020

Influence of CNTs addition on structural and superconducting properties of mechanically alloyed MgB_2

Sigit Dwi YUDANTO[1,2], Yulia Puspa DEWI[3], Perdamean SEBAYANG[4], Septian Adi CHANDRA[2], Agung IMADUDDIN[2], Budhy KURNIAWAN[1], and Azwar MANAF[1,*]

[1] *Department of Physics, Universitas Indonesia, Kampus UI, Depok 16424, Indonesia*
[2] *Research Center for Metallurgy and Materials, Indonesian Institute of Sciences, Gedung 470, South Tangerang, Banten, 15314, Indonesia*
[3] *Department of Materials, Sepuluh Nopember Institute of Technology, Surabaya, East Java, 60111, Indonesia*
[4] *Research Center for Physics, Indonesian Institute of Sciences, Gedung 440, South Tangerang, Banten, Puspiptek, 15314, Indonesia*

[*]**Corresponding author e-mail:** azwar@ui.ac.id

Received date:
6 November 2019
Revised date:
16 April 2020
Accepted date:
8 June 2020

Keywords:
MgB_2
Addition
Carbon nanotubes
Structural
Critical temperature

Abstract

The result of adding carbon nanotubes (CNTs) to the lattice parameters, critical temperature and electrical resistivity of the MgB_2 superconductors is reported. Structurally, the addition of CNTs was found to decrease the *a*-lattice from 3.086 Å of CNTs free sample to 3.078 Å and 3.074 Å of 5% and 10% CNTs added samples due to a substitution of C at the B site which presence in the form of $Mg(B_{1-x}C_x)_2$ main phase. The doping level x of CNTs added samples were 2.25 at% and 3.75 at% respectively. The unreacted CNTs presence as the second phase and further acting as the suppression agent for crystallite growth. The addition of CNTs is also to refine the grain size and improves the grain connectivity. Samples show a metallic behavior which observed only at temperatures above ~41 K, below which, a sharp transition of resistivity occurred toward zero resistivity, confirming the superconductivity behavior. This study concluded that the effect of CNTs addition affects the structural parameters and superconducting properties. The addition of the CNTs to 5% and 10% has changed the zero critical temperature of the sample material to respectively 39.20 and 38.02 K from 39.31 K of CNTs free sample.

1. Introduction

Modern technological products like Mag-Lev trains, magnetic resonance imaging (MRI), ultra-high efficiency electric generators, etc. are already, though being operated under special care and expensive ways. Such products use superconducting magnets or cables to generate high magnetic fields with superior efficiency because a superconductor has a zero resistance. The disadvantage of the existing superconductor when applied in some of such mentioned devices is that it requires cooling media since the critical temperature for most of the superconductors far below room temperature.

Among all existing superconducting candidates, the MgB_2 has been the most promising superconductor for wire applications having a critical temperature of ~39 K [1]. The MgB_2 was introduced in 1953 [2], but its superconductivity behavior was discovered by Jun Akimitsu and his team in 2001 [1]. It is a simple alloy made of Mg and B elements in which the MgB_2 phase has a hexagonal structure with a p63/mmm space group [1]. The MgB_2 possesses a simple crystal structure, made from inexpensive raw materials and having a high critical temperature, not surprisingly the MgB_2 phase immediately received considerable attentions due to its potential for various technological applications. Several studies have focused to improve the superconductivity of the MgB_2. Substitution at the Mg site, B site, or the addition of other elements/ compounds to the MgB_2 has been carried out. Partial substitutions of Ti, Zn, Cu, Al for Mg site [3-6] have been carried out, including the addition of CNTs, nano-carbon, for B site [4,7,8]. Some reports have indicated that the carbon substitution at B site is effective to improve the superconductivity properties [9,10]. The critical current density (J_c) was improved due to very good grain connectivity, although decreasing the critical temperature [9,10]. Such good grain connectivity has enhanced the mass density as well as the density of grain boundaries [11].

Various synthesis techniques for obtaining the MgB_2 phase have been developed to obtain information on the effective synthesis methods to result the MgB_2-based superconductors with enhanced superconductivity properties. Synthesis techniques which have been developed to date include the powder in a sealed tube (PIST) method [12], reactive liquid Mg infiltration (Mg-RLI) [13] solid-state reactions, in situ hot isostatic pressing (HIP) method [6], and so forth. The biggest challenge in the synthesis of the MgB_2 phase lies in the main properties of the Mg element which has a low vapor point and is easily oxidized to form an undesirable MgO phase. In the previous research work [14], we succeeded to suppress the presence of MgO in materials using a combination of high-energy ball milling and

DOI: 10.14456/jmmm.2020.32

PIST methods. Samples prepared by this method have produced MgB_2-based materials with very low levels of MgO i.e. only ~8% MgO is still present in the material. It was demonstrated that samples which sintered at a temperature of 850 and 900°C for 1 h promoted high mass fraction of the MgB_2 phase and critical temperature. However, the porosity and the presence of the second phase are considered still relatively high. Suitable heat treatments as well as optimized material composition are needed to improve the grains connectivity. In the current work, we preserved our synthesis method which applied in the previous work and proven refine the grains and improve the grains connectivity [14-16]. The MgB_2 based materials with the addition of Multi-walled carbon nanotubes (MWCNTs) is brought to be investigated their effects on the crystal structure, microstructure, and critical temperature.

2. Experimental

2.1 CNTs added MgB_2 preparation

MgB_2 + xCNTs (where x = 5 and 10 wt%) samples were prepared through mechanical alloying. Stoichiometric quantities of analytical-grade Mg, B and Multi-Walled CNTs precursors were mixed and milled using a shaker mill for 2 h with an operating speed of 300 rpm. The pre-milled powders and steel balls were inserted into a stainless-steel vial in a glove box while flowing the ultra-high purity argon gas. Then, the milled powder was taken out from the vial to be compacted in a stainless-steel tube. The compacted tube was then sintered in a muffle furnace at 800°C. All samples were heated for 1 h with heating rate 5°C·min^{-1} and left in the furnace to room temperature. The heating process used in this work is somewhat similar to that of our previous work which adopted from Kumar et al. [12,14,17].

2.2 Material characterization

A PANalytical X'Pert MPD diffractometer was employed to determine the crystal structure and phases formed of the samples using Cu Kα radiation (λ = 0.15406 nm). The phase of samples was evaluated in the angle range of 2θ = 10-90°. A quantitative analysis was done by fitting the XRD pattern through the Rietveld method [18]. The mean crystallite size and lattice strain were evaluated graphically from the Williamson-Hall plot (W-H plot) [19]. A JEOL JSM-6390LA Scanning Electron Microscopy (SEM) was used to observe the surface morphology and porosity of the samples. A Cryogenic Magnetometer (Teslatron Cryogenic Magnet equipped with Oxford Instruments) followed by the four-point probe (FPP) method was used to measure the electrical resistivity (ρ) and determination of the critical temperature (Tc) of samples. The electrical resistivity was measured without an applied magnetic field in a temperature range of 5 K to room temperature.

3. Results and discussion

Figure 1 compares the refined X-ray diffraction pattern of MgB_2 samples with the addition of 5 wt% (coded MB 5% CNTs) and 10 wt% (coded MB 10% CNTs) MWCNTs with that of the CNTs free MgB_2 sample (MB 0% CNTs taken from Ref. 14). Inset is plots of enlarged (101) peak for the three samples. MgB_2 phase was identified as the major phase for all samples along with two minor phases Fe_2B, and MgO respectively. However, another diffraction peak at 26.4° was identified in the diffraction pattern of CNTs added samples which suspected to belong to graphite. Fe_2B phase is promoted by the reaction between the steel ball and the boron precursor during the milling process. Such Fe_2B phase presence was also expressed in the previous report, which promoted by a direct reaction between Fe atoms of steel tube and MgB_2 or B during the sintering process at high temperatures [14-16]. No unreacted Mg was observed in the CNTs added MgB_2 samples, which gained credits over sample reported in our previous study [14], in which the X-ray diffraction pattern of pure MgB_2 confirmed the presence of Mg peaks. The mass fraction of unreacted Mg was about 1.6 wt%. In the current work, the peak of Mg has been ascertained absence. Thus, the addition of CNTs to the MgB_2 has optimized the reaction between Mg and B to form the MgB_2 phase. Boron deficiency caused by the formation of MgO and Fe_2B has been compensated by the addition of CNTs during synthesis. In addition, the Bragg position of (101) peak inset shows a shifting, which indicates the CNTs addition cause also a lattice change.

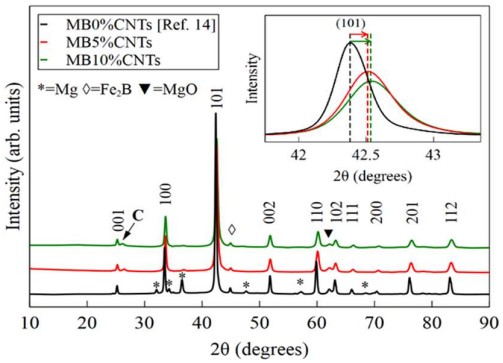

Figure 1. The refined X-ray diffraction pattern of CNTs added samples compared with that of the CNTs free sample.

The values of the full width at half maximum (FWHM) which calculated from (100), (101), (002), (110) and (112) planes in Figure 1 after corrected by instrumental broadening were successively used for calculation of the mean crystallite size in the samples through a W-H plot of Equation 1:

$$\beta_{hkl} \cos \theta = K\lambda/D + 4\varepsilon \sin \theta \quad (1)$$

Where D is the mean crystallite size (nm), K is a dependent constant of crystallite-shape factor (0.9), λ is the wavelength of Cu Kα radiation (0.15406 nm), β_{hkl} is the corrected FWHM value in radians, ε is the micro-strain, and θ is the diffraction angle (°). FWHM value at a (110) peak of MB5% CNTs and MB10% CNTs samples evaluated from a diffraction pattern shown in Figure 1 is respectively 0.5003° and 0.5684°. These values are larger than that of the pure sample (0.3441°) [14], indicate the fine crystallite size. Figure 2 shows the W-H plots of MB0%, MB5% CNTs and MB10% CNTs samples which resulting in the mean crystallite size of 77 nm, 56 nm and 50 nm, respectively. The peak broadening also causes the micro-strain due to lattice distortion of MgB_2 crystallites [8,9].

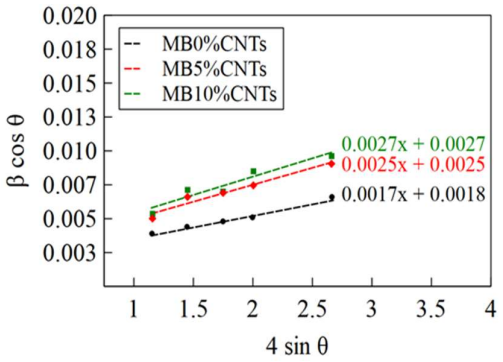

Figure 2. The W-H Plots of CNTs and CNTs added samples for mean crystallite size and micro strain determination.

Table 1 summarizes results of XRD analysis for the three samples along with superconductivity properties which will be discussed later. It shows that the addition of the CNTs has caused a decrease in the *a*-lattice parameter, while that of the *c*-lattice tends to be constant. The *a*-lattice parameter was decreased from 3.086 Å for the CNTs free sample [14] to 3.078 Å for MB5% CNTs and 3.074 Å for MB10% CNTs. A decrease in *a* lattice revealed that there has been a substitution of C at the B site of MgB_2 phase in CNTs added samples [8,20]. Such decrease occurred due to the radius of carbon atom (1.70 Å) is smaller than that of boron (1.92 Å). Hence, the $Mg(B_{1-x}C_x)_2$ would be the main phase in CNTs added samples. This explains an increase in lattice micro-strain of CNTs added MgB_2 samples (see ε value in Table 1). Since there is no change in *c* lattice parameter, the ratio *c/a* increases with an increase of CNTs addition. A change in *c/a* ratio or Δ(*c/a*) of CNTs added samples relative to CNTs free have been used to calculate the doping level (x) of the $Mg(B_{1-x}C_x)_2$ phase [16,21]. The doping level (x) is estimated using the formula $x = 7.5\Delta(c/a)$, where $\Delta(c/a)$ is the change in *c/a* ratio $Mg(B_{1-x}C_x)_2$ compared to pure MgB_2 [14]. The *c/a* ratio of MB5% CNTs and MB10% CNTs is 1.145 and 1.147 respectively (see Table 1) which yielding $\Delta(c/a)$ of 0.003 and 0.005 for respective samples. Hence, referring to such formula, the x value of MB5% CNTs and MB10% CNTs is 2.25 at% (or 1.17 wt%) and 3.75 at% (or 1.96 wt%) respectively. The substituent C atoms are excessively available in both samples which are 5 wt% and 10 wt% respectively. The unreacted CNTs would precipitate at the grain boundary and further acting as the inhibition agent for crystallite growth. This explains finer size of crystallites in CNTs added samples than that of CNTs free sample as listed in Table 1. The decrease of *a*-lattice parameter due to substitution of C together with such precipitates at grain boundary would yield the lattice strain. The micro-strain value of samples was listed in the Table 1.

SEM micrographs of the fracture surface of CNTs free and CNTs added MgB_2 samples are shown successively in Figures 3(a), 3(b) and 3(c). The microstructure shown in Figure 3(a) appears less good grain connectivity, consisting of crystalline grains of platelet shape with inhomogeneous sizes. The size of platelet shape grains as seen in the micrograph is less than 1 μm which 12 times larger than the mean crystallite size (77 nm) evaluated by XRD. In contrast to this, the micrographs shown in Figure 3(b) and 3(c) are featured by fine crystallites morphologies with much better grain connectivity. The grains are fine in sizes and present as massive grain agglomerates. Even the microstructure with much denser agglomerates due to fine crystallites can be seen in Figure 3(c). Referring to Table 1, the mass fraction of CNTs added samples are greater than that of the CNTs free sample. It implies that the addition of CNTs to the MgB_2 has increased the mass fraction of the MgB_2 phase, and improved grain connectivity when compared with that of the CNTs free MgB_2 sample.

Figure 4 compares plots of resistivity vs temperature of the CNTs added samples with that of CNTs free. These plots clearly demonstrate that all samples show a superconductive state. The CNTs added samples show a metallic behavior only at temperatures above ~41 K, below which, a sharp transition of resistivity occurred toward zero resistivity, confirming the superconducting behavior. The temperature at which a transition to zero state is known as the onset critical temperature (Tc_{onset}). Referring to the plots of the temperature dependence of the resistivity in Figure 4, the value of MB5% CNTs sample increases continuously from 351.14 μΩ·cm at its respective Tc_{onset} to 592.45 μΩ·cm at 275 K. Whereas, that of the MB10% CNTs sample increased from 265.77 μΩ·cm to 392.79 μΩ·cm at 275 K. Hence, the temperature dependence of the resistivity for the two samples in the metallic state is different because the two samples have different mass fraction of main phase. A ratio between the resistivity value at 275 K and Tc_{onset} determines the residual resistivity ratio (RRR) [22], we found that the RRR value decrease with increasing of CNTs content. RRR is defined as the ratio $\rho_{(275K)}/\rho_{(onset)}$. The resistivity increases with increasing amount of impurities and defects present in the materials. Hence, a decrease in RRR value means the defects and impurities in superconductor are increased. The presence of the unreacted carbon in the CNTs added samples confirms such defects exist.

Table 1. Resume of refined XRD pattern data, crystallite size, electrical resistivity and critical temperature of samples.

Source	MB0% CNTs	MB5% CNTs	MB10% CNTs
FWHM of (100) (degree)	0.2462	0.3108	0.3310
FWHM of (101) (degree)	0.2850	0.4141	0.4453
FWHM of (002) (degree)	0.3191	0.4476	0.4531
FWHM of (110) (degree)	0.3441	0.5003	0.5684
FWHM of (112) (degree)	0.5127	0.6991	0.7426
Crystallite size (nm)	77	56	50
Micro-strain (ε)	0.0017	0.0025	0.0027
Mass fraction of MgB_2 phase (%)	89.94 [14]	91.32	89.18
a-axis constant (Å)	3.086 [14]	3.078	3.074
c-axis constant (Å)	3.525 [14]	3.525	3.525
c/a	1.142 [14]	1.145	1.147
x (CNTs content, at%)	0	2.25	3.75
$\rho_{275\ K}$ (μΩ·cm)	509.66 [14]	592.45	392.79
ρ_{onset} (μΩ·cm)	194.46 [14]	351.14	265.77
Residual Resistivity Ratio (RRR)	2.34 [14]	1.69	1.48
Tc_{onset} (K)	41.65 [14]	41.05	40.09
Tc_{zero} (K)	39.31 [14]	39.20	38.02

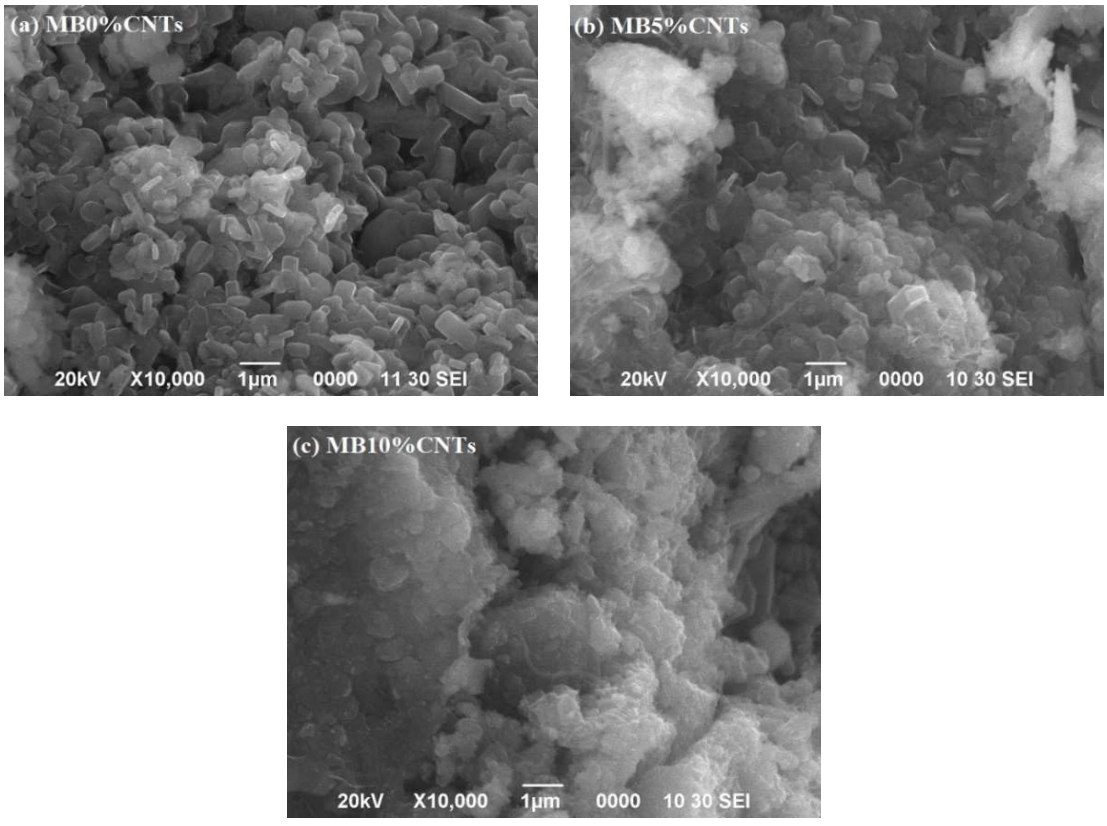

Figure 3. SEM micrographs of the fracture surface of (a) CNTs free, (b) MB5% CNTs and (c) MB10% CNTs samples.

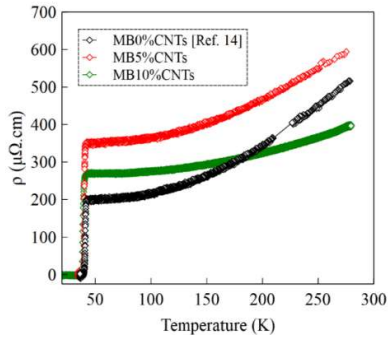

Figure 4. Temperature dependence of resistivity curves of CNTs free and CNT added samples.

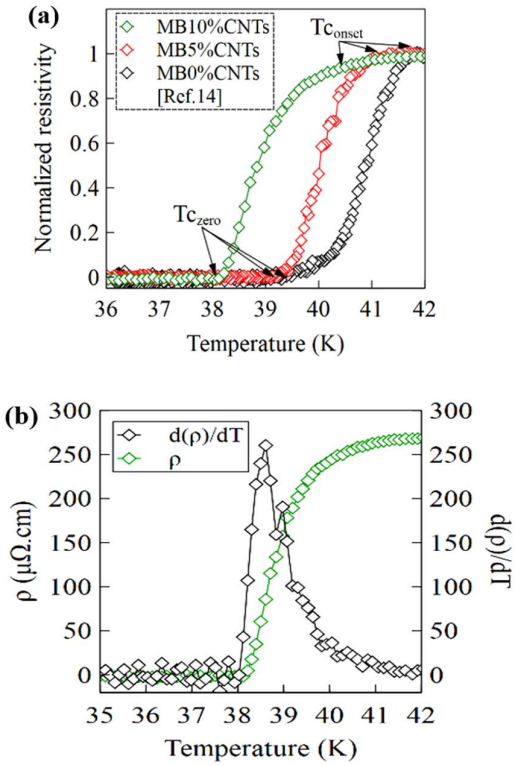

Figure 5. (a) Curves of resistivity value in the temperature range of superconductive to conductive state for CNTs free and added samples. A typical resistivity curve vs temperature and its corresponding first-order derivative of the CNTs added sample (b).

One of the most wanted parameters expected from a superconductor is the zero critical temperature (Tc_{zero}) at which the resistivity at temperatures below Tc_{zero} is theoretically zero. The Tc_{zero} is derived from the first-order derivative of temperature dependence of the resistivity. Plots of resistivity value in the temperature range of conductive to superconductive state for the three samples are shown in Figure 5(a). Obviously, the three samples have a different temperature transition. A typical resistivity plot vs temperature and its corresponding first-order derivative of the CNTs added sample is shown in Figure 5(b) from which the Tc_{onset} and Tc_{zero} are derived. The resulting values were respectively 41.05 K and 39.2 K for MB5% CNTs. Whereas for MB10% CNTs, Tc_{onset} and Tc_{zero} are respectively 40.09 K and 38.02 K. Such values are smaller than that of CNTs free sample sintered at 800°C for 1 h, which showed the superconducting state with the Tc_{onset} and Tc_{zero} of 41.65 K and 39.31 K, respectively [14]. Hence, the addition of MWCNTs in MgB_2 superconductor decreased the Tc_{onset} and Tc_{zero}. Our current finding is in good agreement with results that reported previously [7,8,20].

4. Conclusions

In this study, superconductor of the MgB_2 phase with the addition of CNTs has been successfully synthesized. The addition of CNTs during the synthesis of MgB_2 affects the structural, morphological and superconducting properties. The *a*-lattice of the MgB_2 phase is decreased by carbon substitution the boron at boron site. The excess CNTs in the CNTs added samples would fall at the grain boundary acting as the grain refiner. CNTs precipitates together with lattice distortion promote the lattice strain. The addition of CNTs to the MgB_2 has increased the mass fraction of the MgB_2 phase, and improved grain connectivity. The Tc_{zero} values in the MB5% CNTs and MB10% CNTs sample were 39.20 and 38.02 K, respectively.

5. Acknowledgements

We are thankful for the financial support provided by the Directorate of Research and Community Service Universitas Indonesia under program Grants of International Publication Indexed 9 (PIT 9, 2019) under contract No. NKB-002/UN2.R3.1/HKP.05.00/2019. The authors gratefully acknowledge the support of the Postgraduate Program of Materials Science Universitas Indonesia and the Metallurgical Research Centre, Indonesian Institute of Science, the Ministry of Research, Technology and Higher Education for the research facilities.

References

[1] J. Nagamatsu, N. Nakagawa, T. Muranaka, Y. Zenitani, and J. Akimitsu, "Superconductivity at 39 K in magnesium diboride," *Nature*, vol. 410, pp. 63-64, 2001.

[2] M. E. Jones and R. E. Marsh, "The preparation and structure of magnesium boride, MgB_2," *Journal of The American Chemical Society*, vol. 76, pp. 1434-1436, 1954.

[3] F. Yang, S. Q. Li, G. Yan, J. Q. Feng, X. M. Xiong, S. N. Zhang, Q. Y. Wang, G. Q. Liu, Y. C. Pang, H. F. Zou, C. S. Li, and Y. Feng, "Improved superconducting properties in Ti-doped MgB_2 prepared by two-step reaction method and high-energy ball milling," *Journal of Alloys and Compounds*, vol. 622, pp. 714-718, 2015.

[4] A. Y. Potanin, D. Y. Kovalev, E. A. Levashov, P. A. Loginov, E. I. Patsera, N. V. Shvyndina, K. S. Pervakov, V. A. Vlasenko, and S. Y. Gavrilkin, "The features of combustion synthesis of aluminum and carbon doped magnesium diboride," *Physica C*, vol. 541, pp. 1-9, 2017.

[5] A. Y. Potanin, D. Y. Kovalev, Y. S. Pogozhev, and N. Y. Khomenko, "Metal-doped MgB_2 by thermal explosion: A TRXRD study," *International Journal of Self-Propagating High-Temperature Synthesis*, vol. 27, pp. 18-25, 2018.

[6] T. Naito, T. Yoshida, H. Mochizuki, H. Fujishiro, R. Basu, and J. A. Szpunar, "Vortex pinning properties of dense Ti-doped MgB_2 Bulks sintered at different temperatures," *IEEE Transactions on Applied Super-conductivity*, vol. 26, no. 3, pp. 1-5, 2016.

[7] G. Serrano, A. Serquis, L. Civale, B. Maiorov, T. G. Holesinger, F. Balakirev, and M. Jaime, "Single-wall carbon nanotubes addition effects on the superconducting properties of MgB_2," *International Journal of Modern Physics B*, vol. 23, pp. 3465-3469, 2009.

[8] J. H. Lim, C. M. Lee, J. H. Park, J. H. Choi, J. H. Shim, J. Joo, Y. H. Lee, W. N. Kang, and C. J. Kim, "Doping effect of CNT and nanocarbon in magnesium diboride bulk," *Journal of Nano-science and Nanotechnology*, vol. 9, pp. 7388-7392, 2009.

[9] J. H. Kim, W. K. Yeoh, M. J. Qin, X. Xu, and S. X. Dou, "The doping effect of multiwall carbon nanotube on MgB_2/Fe superconductor wire," *Journal of Applied Physics*, vol. 100, pp. 1-6, 2006.

[10] R. H. T. Wilke, S. L. Bud, P. C. Canfield, D. K. Finnemore, and R. J. Suplinskas, "Systematic effects of carbon doping on the superconducting properties of $Mg(B_{1-x}C_x)_2$," *Physical Review Letters*, vol. 92, pp. 217003, 2004.

[11] Y. Shimada, S. Hata, K. I. Ikeda, H. Nakashima, S. Matsumura, H. Tanaka, A. Yamamoto, J. I. Shimoyama, and K. Kishio, "Microstructural connectivity in sintered ex-situ MgB_2 bulk superconductors," *Journal of Alloys and Compounds*, vol. 656, pp. 172-180, 2016.

[12] R. G. A. Kumar, K. Vinod, R. P. Aloysius, and U. Syamaprasad, "A simple and inexpensive method for rapid synthesis of MgB_2 super-conductor," *Materials Letters*, vol. 60, pp. 3328-3331, 2006.

[13] A. G. Bhagurkar, A. Yamamoto, A. R. Dennis, J. H. Durrell, T. A. Aljohani, H. B. Nadendla, and D. A. Cardwell, "Microstructural evolution in infiltration-growth processed MgB_2 bulk superconductors," *Journal of the American Ceramic Society*, vol. 100, pp. 2451-2460, 2017.

[14] S. D. Yudanto, Y. P. Dewi, A. Imaduddin, Y. Nakanishi, M. Yoshizawa, B. Kurniawan, and A. Manaf, "Improvement in the crystallographic phase content and superconducting properties of mechanically alloyed MgB_2," *Journal of Superconductivity and Novel Magnetism*, vol. 32, pp. 2829-2835, 2019.

[15] B. Jun, J. Ho, C. Kim, and K. Nam, "Improved transport critical current properties in glycerin-doped MgB_2 wire using milled boron powder and a solid-state reaction of 600°C," *Journal of Alloys and Compounds*, vol. 650, pp. 794-798, 2015.

[16] B. H. Jun, Y. J. Kim, K. S. Tan, and C. J. Kim, "Effective carbon incorporation in MgB_2 by combining mechanical milling and the glycerin treatment of boron powder," *Superconductor Science and Technology*, vol. 21, pp. 105006, 2008.

[17] A. Imaduddin, S. D. Yudanto, M. E. H. Rasyadi, Y. Nakanishi, and M. Yoshizawa, "Possibility of the higher critical temperature on MgB_2 superconductor synthesized by powder-in-sealed-tube method," *Journal of Low Temperature Physics*, vol. 195, pp. 460-473, 2019.

[18] A. C. Larson and R. B. Von Dreele, "General structure analysis system (GSAS)," 2004.

[19] H. Irfan, K. Mohamed Racik, and S. Anand, "Microstructural evaluation of $CoAl_2O_4$ nano-particles by Williamson–Hall and size–strain plot methods," *Journal of Asian Ceramic Societies*, vol. 6, pp. 54-62, 2018.

[20] S. X. Dou, W. K. Yeoh, J. Horvat, and M. Ionescu, "Effect of carbon nanotube doping on critical current density of MgB_2 superconductor," *Applied Physics Letters*, vol. 83, pp. 4996-4998, 2003.

[21] A. Vajpayee, V. P. S. Awana, G. L. Bhalla, P. A. Bhobe, A. K. Nigam, and H. Kishan, "Super-conducting properties of adipic-acid-doped bulk MgB_2 superconductor," *Super-conductor Science and Technology*, vol. 22, pp. 015016, 2009.

[22] S. R. Chauhan and S. Chaudhary, "On the residual resistivity ratio in MgB_2 super-conductors," *IEEE Transactions on Applied Superconductivity*, vol. 20, pp. 26-32, 2010.